

# Effect of Hot Corrosion on the Creep Properties of Types 321 and 347 Stainless Steels

J.G. González-Rodríguez, A. Luna-Ramírez, and A. Martínez-Villafañe

(Submitted 18 July 1997; in revised form 14 September 1998)

Problems caused by hot corrosion and creep damage on superheater and reheater tubes of power plants using heavy oil as fuel inhibit the continuous service of the boilers and shorten their design lives. The acceleration of hot corrosion attack of boilers is caused by the presence of fuel ash deposits containing V, Na, and S, in the form of  $\text{Na}_2\text{SO}_4$  and  $\text{V}_2\text{O}_5$ , which form low melting point phases. In addition to this, the tubes are exposed to the action of both high stresses and high temperatures, producing a continuous plastic deformation of the tube walls called creep damage. Creep rupture tests were carried out in the temperature range 620 to 670 °C in static air in the presence of corrosive environments using 321H and 347H type stainless steels used in superheater and reheater tubes under hot corrosion and creep environments. The corrosive environment includes synthetic  $\text{Na}_2\text{SO}_4$ ,  $\text{V}_2\text{O}_5$ , and the mixture 80%  $\text{V}_2\text{O}_5$ -20%  $\text{Na}_2\text{SO}_4$ . Also, the role of the different elements present in the environments on corrosion was investigated using electronic microscopy and x-ray diffraction techniques.

**Keywords** creep, hot corrosion, stainless steel type 321H, stainless steel type 347H

## 1. Introduction

Components used in boiler heat exchangers, especially in superheaters (SH) and reheaters (RH) are subjected to chemically aggressive environments at elevated temperatures in addition to the mechanical stresses that they bear in service conditions. The mechanical stresses give rise to creep deforma-

tion. Though the tube materials of boiler SH and RH are designed for sufficient life against creep damage, the original design life cannot be achieved. These problems are caused by creep damage and tube wall thinning due to hot corrosion (Ref 1). On the other hand, the heavy oil used as boiler fuel contains impurities such as vanadium, silicon, and sodium, which form low melting point phases promoting hot corrosion reactions, consequently shortening the life of boiler tube materials. Eventually, phenomenological aspects of these problems at the tube surface of boilers (at the fireside) can be classified as wall thinning due to hot corrosion by flue ash attack and the creep damage.

Some important ways in which hot corrosion lowers the mechanical properties are by reduction of the load-bearing cross-sectional area (Ref 2), production of voids at the grain boundaries by outward diffusion of metal ions (Ref 3), and formation of low-melting eutectics at the surface, which exposes the metal directly to aggressive environments. Therefore, hot corrosion is an important practical phenomenon not only in

**J.G. González-Rodríguez**, Facultad de Ciencias Químicas e Ingeniería, Universidad Autónoma del Estado de Morelos, Av. Universidad 1001, Cuernavaca, Mor., México; **A. Luna-Ramírez**, Instituto de Investigaciones Eléctricas, Departamento de Equipos Mecánicos Rotatorios, Av. Reforma 113, 62490-Temixco, Mor., México; and **A. Martínez-Villafañe**, Centro de Investigaciones en Materiales Avanzados, León Tolstoi 166, Complejo Industrial Chihuahua, 31109-Chihuahua, Chih., México.

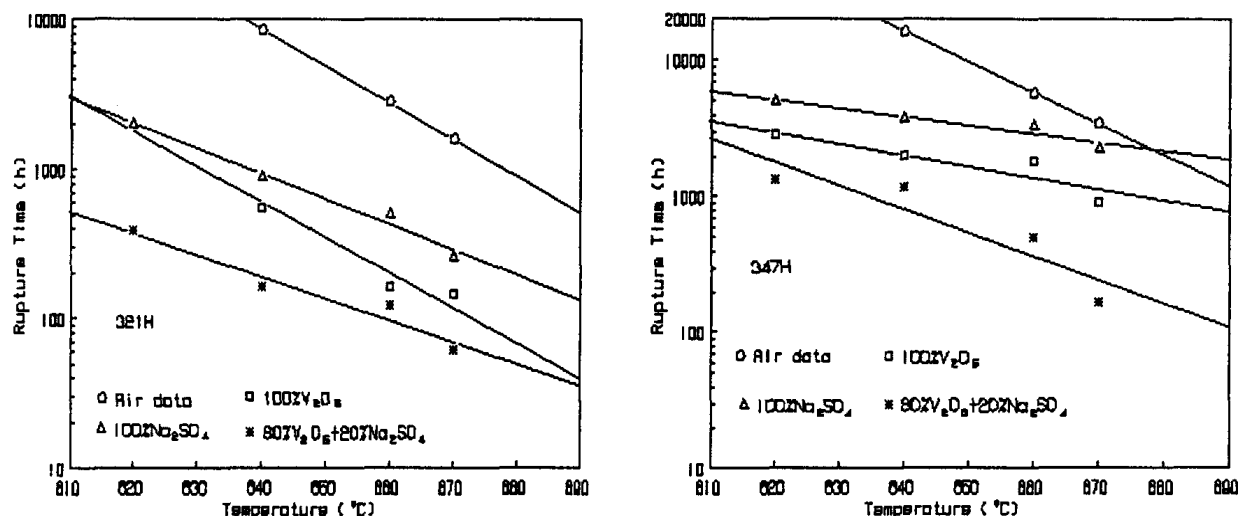
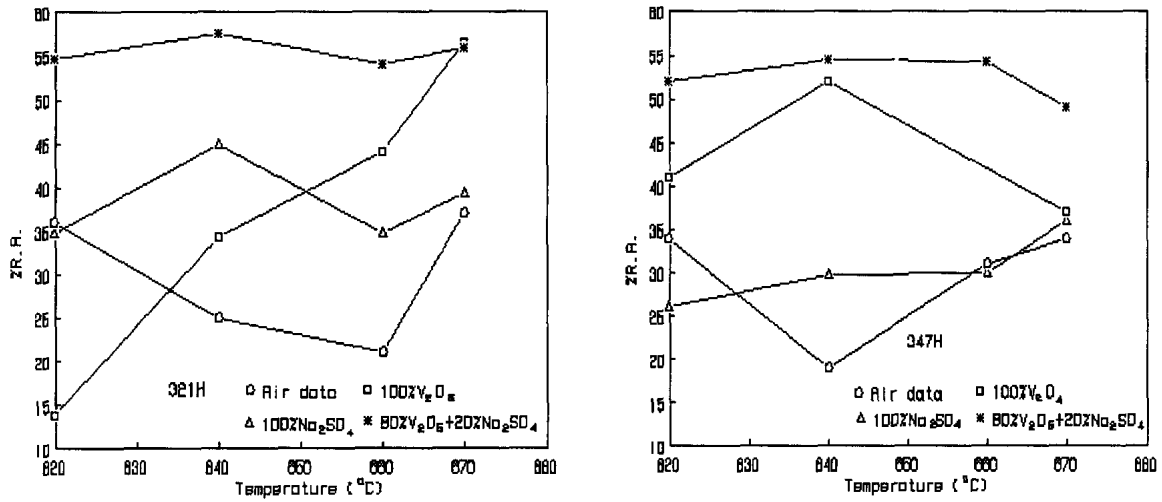


Fig. 1 Variation of rupture time with temperature for 321H and 347H steels in different environments at a stress value of 14 kg/mm<sup>2</sup>

boilers but also in various elevated temperature applications such as jet, gas turbine, and diesel engines. Until now, the hot corrosion and elevated temperature strength have been treated

separately as independent research fields, and the performance of high temperature materials in service is usually decided on the basis of either hot corrosion resistance or mechanical prop-



**Fig. 2** Variation of percentage reduction in area (% RA) with temperature for 321H and 347H steels in different environments at a stress value of 14 kg/mm<sup>2</sup>

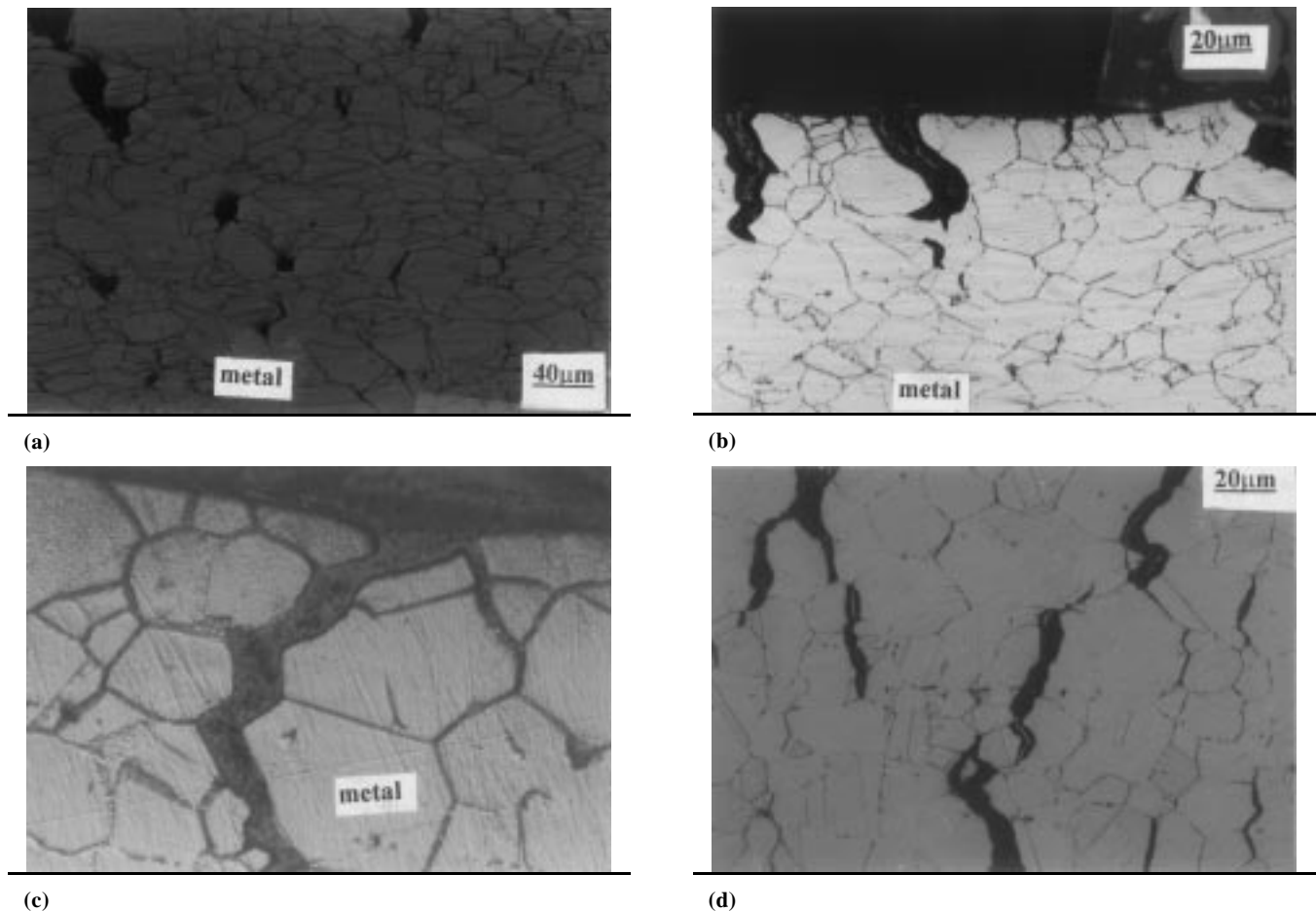


**Fig. 3** Micrographs showing cracks on the surface of 321 type stainless steel creep tested in (a) air, (b) 100% Na<sub>2</sub>SO<sub>4</sub>, (c) 100% V<sub>2</sub>O<sub>5</sub>, and (d) 80% V<sub>2</sub>O<sub>5</sub> + 20% Na<sub>2</sub>SO<sub>4</sub>

erties. However, in actual service conditions, the material will experience both hot corrosion and creep simultaneously. Thus, this article reports a study of the prediction of the creep life of type 321H and 347H stainless steels, commonly used as tube materials of boiler superheaters and reheaters in hot corrosion environments.

## 2. Experimental

The chemical composition of the materials used in this work are given in Table 1, which are under specification. Flat creep specimens with a 30.0 mm gage length and 2.0 by 3.2 mm in the

reduced cross section were machined from unused tubes. Prior to testing, the specimens were abraded along their axes with 120 emery paper, degreased with acetone and coated uniformly with  $5 \text{ kg/m}^2$  of either  $\text{Na}_2\text{SO}_4$ ,  $\text{V}_2\text{O}_5$ , or the mixture  $80\% \text{ V}_2\text{O}_5 + 20\% \text{ Na}_2\text{SO}_4$ . The creep experiments were carried out over a range temperature of 620 to 670 °C stainless steel using a constant stress of  $14 \text{ kg/mm}^2$  in an 8:1 lever type creep testing machine. The temperature of the specimen surface along its axis was kept within  $\pm 2 \text{ }^\circ\text{C}$ , and the temperature fluctuation during the test was within about  $\pm 2 \text{ }^\circ\text{C}$ . After failure, the specimens were mounted in bakelite and observed in a scanning electronic microscope, and the scales of the fractured specimens were identified by x-ray diffraction.

**Table 1** Chemical composition of 321H and 347H stainless steels

Steel	Chemical composition, wt%							
	Cr	Ni	Mn	C	Si	Ti	Nb	Fe
321H	18.5	13.6	1.8	0.09	0.7	0.36	...	bal
ASTMA213-75	17 to 19	9 to 12	2.0	0.08	1.0	0.40	...	bal
347H	18.1	11.3	1.9	0.08	0.66	...	0.85	bal
ASTMA213-75	17 to 19	9 to 13	2.0	0.08	1.0	...	0.80	bal

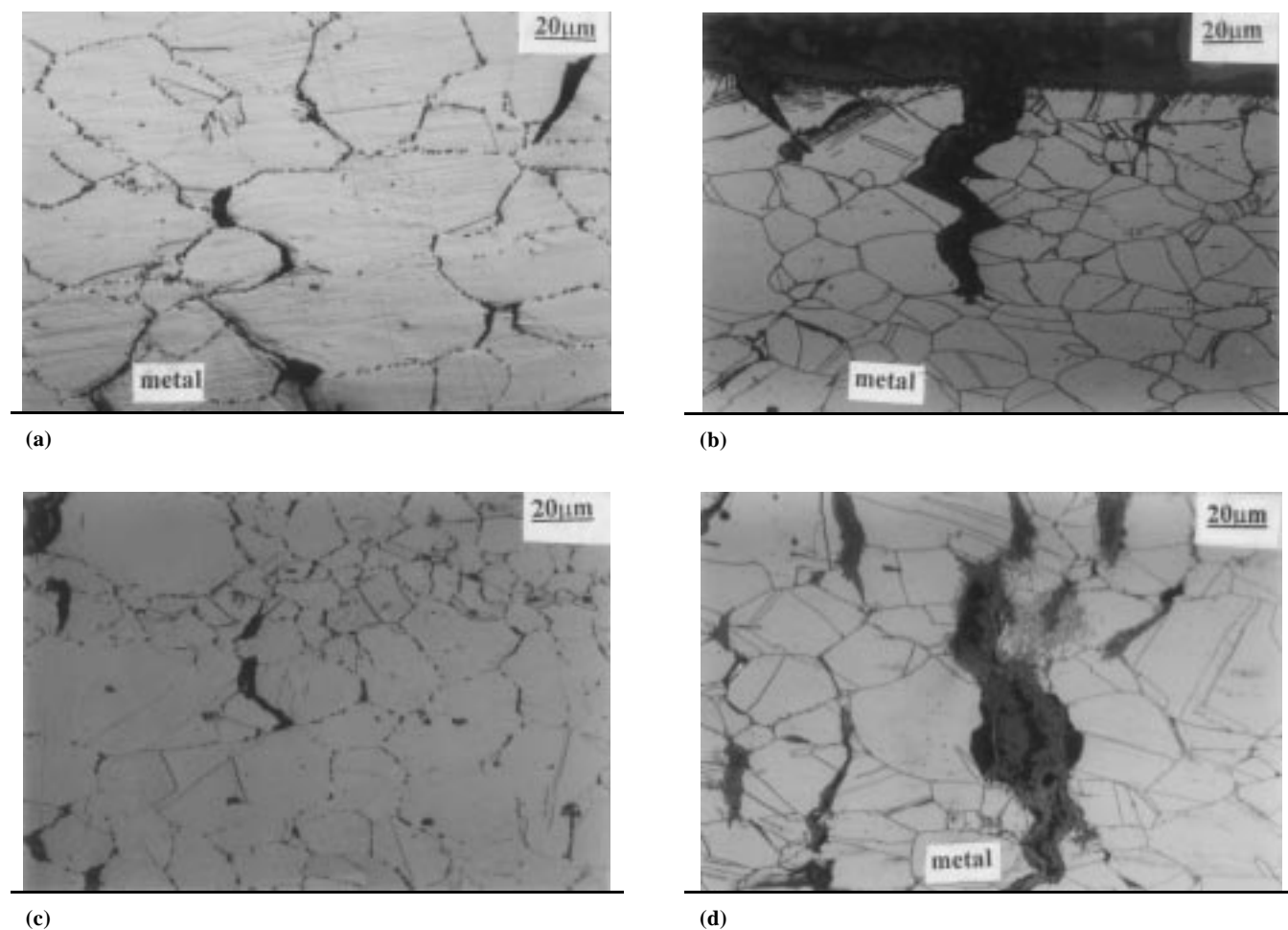
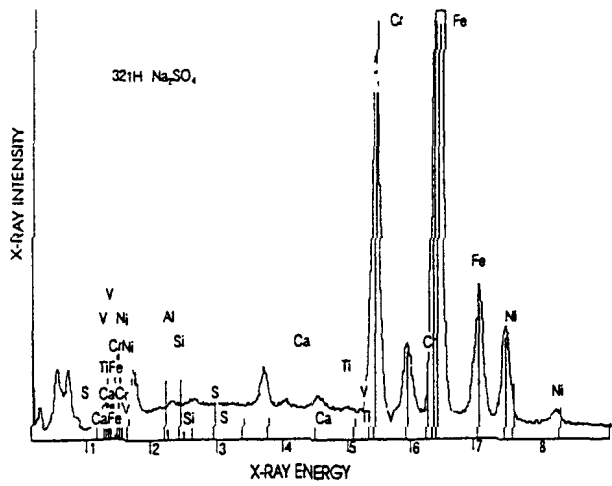
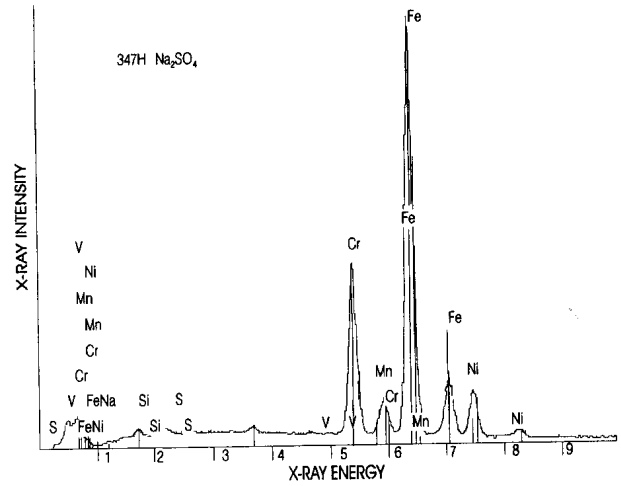


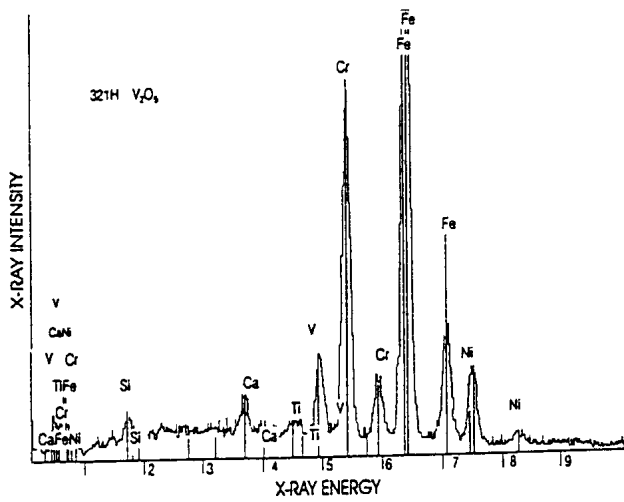
**Fig. 4** Micrographs showing cracks on the surface of 347 type stainless steel creep tested in (a) air, (b) 100%  $\text{Na}_2\text{SO}_4$ , (c) 100%  $\text{V}_2\text{O}_5$ , and (d) 80%  $\text{V}_2\text{O}_5 + 20\% \text{ Na}_2\text{SO}_4$



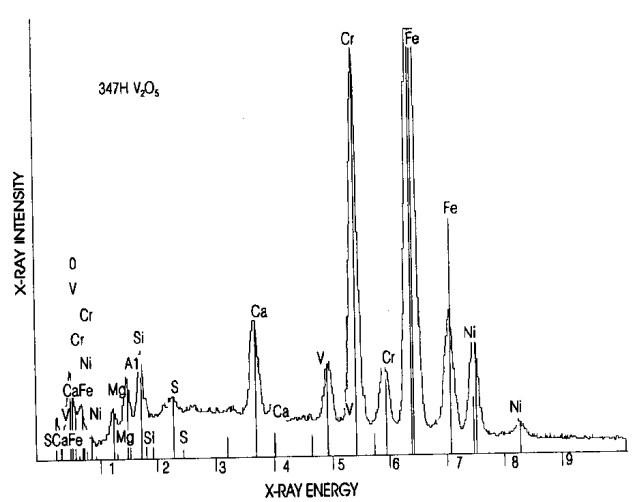
(a)



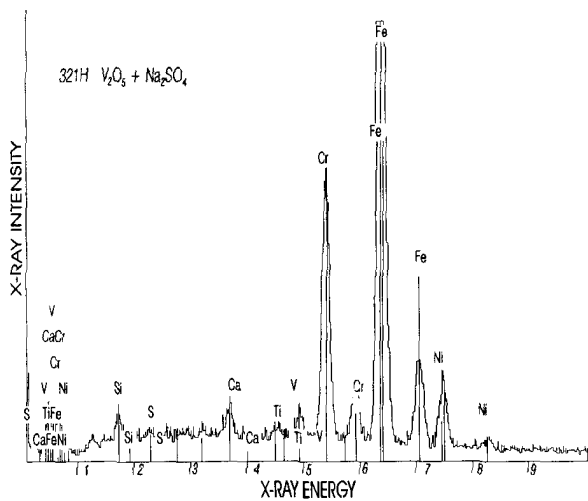
(a)



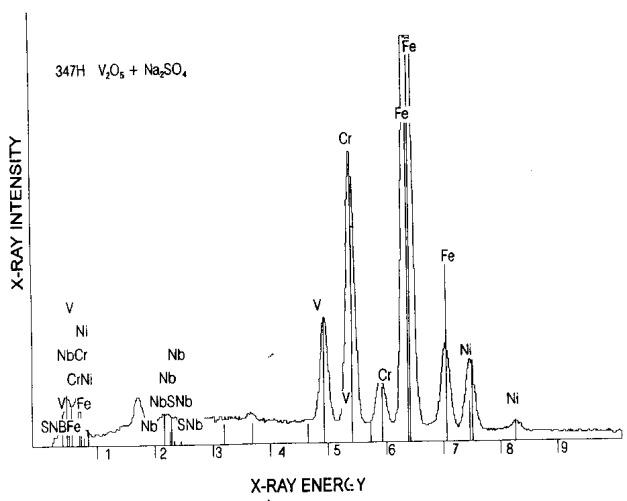
(b)



(b)



(c)



(c)

**Fig. 5** EDX spectra done inside a crack of 321H steel fractured in (a)  $\text{Na}_2\text{SO}_4$ , (b)  $\text{V}_2\text{O}_5$ , and (c) 80%  $\text{V}_2\text{O}_5$  + 20%  $\text{Na}_2\text{SO}_4$

**Fig. 6** EDX spectra done inside a crack of 347H steel fractured in (a)  $\text{Na}_2\text{SO}_4$ , (b)  $\text{V}_2\text{O}_5$ , and (c) 80%  $\text{V}_2\text{O}_5$  + 20%  $\text{Na}_2\text{SO}_4$

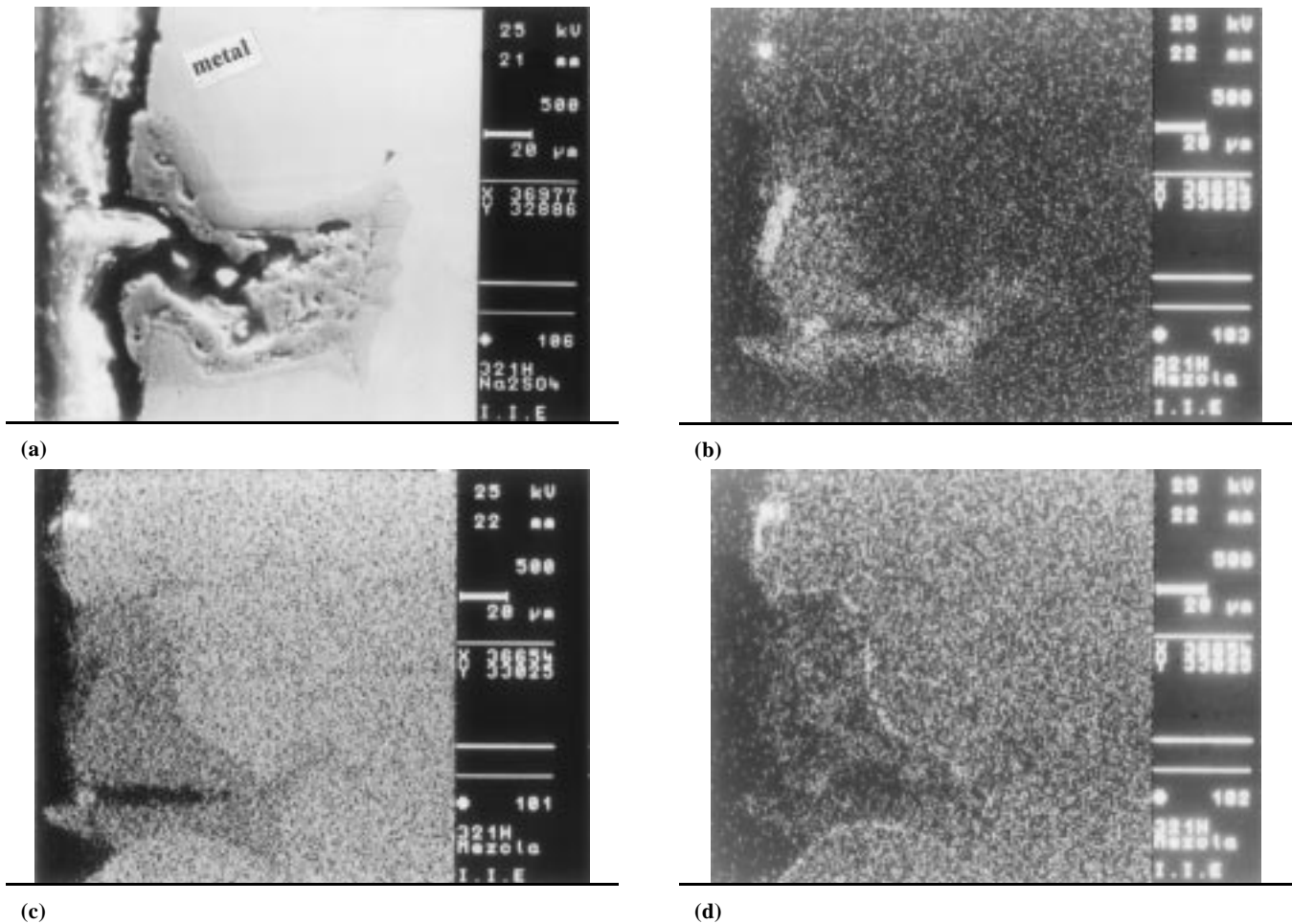


Fig. 7 Elemental mapping of V, Fe, and Ni in 321 steel creep tested in 80%  $V_2O_5$  + 20%  $Na_2SO_4$

**Table 2** Corrosion products found in the creep tested 321H steel

Temperature, °C	Corrosion products found in specimen tested in $V_2O_5$	Corrosion products found in specimen tested in 80% $V_2O_5$ + 20% $Na_2SO_4$
640	...	$FeCr_2O_4$ , $Ni_3S_2$ , NiS, FeS, NiO, $FeV_2O_4$ , $Fe_2O_3$
660	$V_2O_5$ , $Fe_2O_3$ , FeO, $Ni_3V_2O_8$ , $Ni_2V_2O_7$	$FeCr_2O_4$ , $Ni_3S_2$ , FeS, NiO, $Fe_2O_3$ , $Ni_3V_2O_8$
670	$V_2O_5$ , $Fe_2O_3$ , FeO, $Ni_3V_2O_8$ , $Ni_2V_2O_7$	$FeV_2O_4$ , $Ni_3S_2$ , $FeVO_4$ , $Fe_2O_3$ , $Ni_3V_2O_8$ , $CrS_4$

**Table 3** Corrosion products found in the creep tested 347H steel

Temperature, °C	Corrosion products found in specimen tested in $V_2O_5$	Corrosion products found in specimen tested in 80% $V_2O_5$ + 20% $Na_2SO_4$
620	$FeV_2O_4$ , $FeVO_4$	$Cr_2O_3$ , $V_2O_5$ , NiO, $FeV_2O_4$
640	$Fe_2O_3$ , $FeCr_2O_4$ , $V_2O_5$	$Fe_2O_3$ , $Ni_3V_2O_8$ , $Cr_3S_4$
660	$V_2O_5$ , $Fe_2O_3$ , $FeV_2O_4$ , $FeVO_4$ , $FeCr_2O_4$	$FeCr_2O_4$ , $Ni_3S_2$ , NiO, $Fe_2O_3$ , $Ni_3V_2O_8$ , $FeV_2O_4$ , $V_2O_5$
670	$V_2O_5$ , $Fe_2O_3$ , NiO, $FeV_2O_4$ , $FeCr_2O_4$	$FeV_2O_4$ , $FeCr_2O_4$ , $FeV_2O_4$ , $Ni_3V_2O_8$ , $CrS_4$ , $Ni_3S_2$ , $V_2O_5$

### 3. Results

Figure 1 shows the relationship between rupture time,  $t_r$ , and temperature,  $T$ , on a semi-log scale for both steels in air, 100%  $Na_2SO_4$ , 100%  $V_2O_5$ , and the 80%  $V_2O_5$  + 20%  $Na_2SO_4$  mixture at 14 kg/mm<sup>2</sup>. The rupture times in the mixture are the shortest ones. The rupture times in 100%  $Na_2SO_4$  (wt%) are the lowest ones for the three corrosive environments. In this range of temperature, the severity of the 100%  $Na_2SO_4$  attack is not

very great, but the 100%  $V_2O_5$  and the mixture attack more quickly, resulting in severe tube life reduction. In all cases it can be seen that the 347H type stainless steel performs better, perhaps because the stabilizing element is higher for this steel (0.85% Nb) than for the 321H steel (0.36% Ti).

Figure 2 shows the relation between the percentage reduction in area (%RA) with temperature for both steels. It can be seen that in both cases the largest reductions in cross sectional area were obtained in the 80%  $V_2O_5$  + 20%  $Na_2SO_4$  mixture

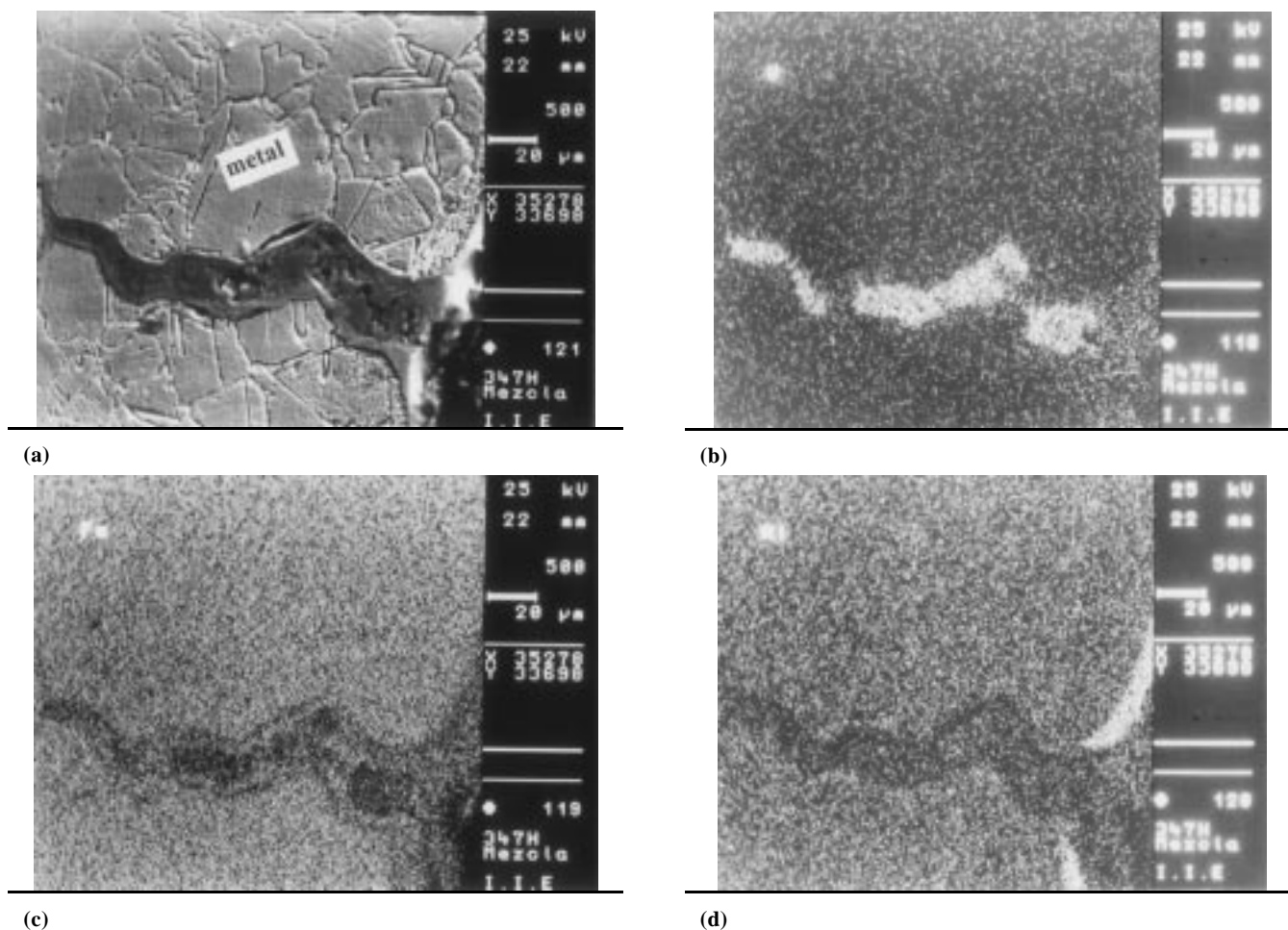


**Fig. 8** Elemental mapping of V, Fe, and Ni in 347 steel creep tested in 80%  $V_2O_5$  + 20%  $Na_2SO_4$

and the smallest values were obtained in 100%  $Na_2SO_4$ . The specimens always showed intergranular fractures (Fig. 3, 4). For the steels fractured in 100%  $Na_2SO_4$ , oxides were found inside the cracks rather than deposits, unlike the specimens fractured in 100%  $V_2O_5$  or the 80%  $V_2O_5$  + 20%  $Na_2SO_4$  mixture, where V-containing deposits were found inside the cracks (as shown in the electron dispersive analysis by x-ray [EDX] spectra, Fig. 5 and 6). The EDX spectra indicate that the deposits penetrated the steel, and this was confirmed by elemental mapping of V, Fe, and Ni (Fig. 7 and 8). The compounds identified from the x-ray analysis of corrosion products in the two steels are shown in Tables 2 and 3.

#### 4. Discussion

The fracture of materials under creep conditions is due to the nucleation and growth of grain boundary cavities. The presence of a corrosive environment such as 100%  $Na_2SO_4$  inside the grain boundaries will increase the damage. However, for the corrosive environment to diffuse into the material, it must be in a liquid form. The  $Na_2SO_4$  melting point is around 850 °C, so at the temperatures used in this work, this compound is in a solid form. Therefore it should not affect the creep properties of

the material. In fact, the times to rupture in air of the two steels used in this work were not as different in this environment as those obtained in air. The EDX analysis did not reveal the presence of sulfur in the steel, indicating that the corrosive environment did not penetrate into the materials.

On the other hand, the  $V_2O_5$  melting point is 665 °C, and the mixture 80%  $V_2O_5$  + 20%  $Na_2SO_4$  melts at 615 °C, indicating that this material was liquid at the test temperature (620 to 670 °C), dissolves the oxide, and possibly penetrates the steel. The EDX results of the specimens tested in these two environments showed the presence of vanadium along the grain boundaries, inducing shorter creep rupture times than those in air for both steels. Ahila (Ref 4) showed that ternary systems such as  $V_2O_5$ -NiO- $Cr_2O_3$  and  $Fe_2O_3$ - $V_2O_5$ - $Cr_2O_3$  can be in a liquid state at temperatures as low as 550 and 480 °C. In the present work, compounds such as NiO,  $Cr_2O_3$ ,  $Fe_2O_3$ ,  $FeVO_4$ , and  $Fe_2O_4$  were detected in the scales of the fractured specimens (Tables 2 and 3). Under some circumstances, dissolution of protector oxides can take place due to the formation of eutectics as in the case of the  $V_2O_5$ . When  $Na_2SO_4$  is added to the vanadium pentoxide, vanadium reacts with iron to form vanadates such as  $FeVO_4$  and  $FeV_2O_4$ , whereas sulfur reacts with iron and nickel to form sulfides such as  $FeS_2$  and  $Ni_3S_2$  with low melting points (lower than 635 °C). Degradation of

the salt-coated samples is attributed to the fluxing of the protective oxide scale by the salt deposits which are liquid at the test temperatures and to easier crack nucleation in the presence of a liquid deposit at the grain boundaries. Penetration of the liquid phase at the grain boundaries and cavity formation due to creep enhanced crack propagation, which are aided by the presence of an applied stress and by surface crack propagation, become easier in the presence of liquid deposits. The liquid deposits further enhance the diffusion of corrosive species. Thus, the observed degradation of creep-rupture properties can be explained as a result of a synergistic action of corrosion and mechanical stress. In the presence of stress, the mobility of the corrosive species may be enhanced, although it is not needed. An increase in temperature increased the degree of degradation due to increase in fluidity of the corrosive melt and the increased diffusion rate at the highest temperatures.

## 5. Conclusions

- $\text{Na}_2\text{SO}_4$  did not have a significant effect on the creep properties of either 321H or 347H type stainless steels in the temperature range 620 to 670 °C.
- $\text{V}_2\text{O}_5$  had an appreciable effect on the creep properties of both 321H and 347H type stainless steels. It did penetrate the steels grain boundaries due to its low melting point and the formation of eutectics like  $\text{V}_2\text{O}_5\text{-NiO-Cr}_2\text{O}_3$  and  $\text{Fe}_2\text{O}_3\text{-V}_2\text{O}_5\text{-Cr}_2\text{O}_3$ , which melt at 550 and 480 °C.
- The addition of sodium sulfate to the vanadium pentoxide increased the aggressive nature of the deposits due to the formation of compounds such as  $\text{FeVO}_4$ ,  $\text{FeV}_2\text{O}_4$ ,  $\text{FeS}_2$ , and  $\text{Ni}_3\text{S}_2$ , which penetrate into the steel faster in the presence of mechanical stresses and corrode the grain boundaries.

## References

1. J.D. Parker, "Boiler Tube Failures in Fossil Power Plants," EPRI Report No. EPRI CS-5500-SR, Atlanta GA, 1987, p 3-73
2. V. Suryanayaranan, K.J.L. Iyer, and V.M. Radhakrishnan, *Mater. Sci. Eng. A*, Vol 112, 1989, p 107-116
3. P. Kofstad, *Proceedings of the Symposium on High Temperature Corrosion in Coal Gasification Atmosphere* J.F. Norton, Ed., Elsevier, London, 1984, p 207-222
4. S. Ahila, S. Ramakrishna, and V.M. Radhakrishnan, *Trans. Indian Institute of Metals*, Vol 46 (No. 4), 1993, p 215-223